Investigation of the power coupling of novel wavelength-selective couplers incorporating axially symmetric long-period fibre gratings

Authors:
Ronnie Kritzinger[1]
Johan Meyer[1]
Johan Burger[2]

Affiliations:
[1]Department of Electrical and Electronic Engineering Science, University of Johannesburg, Johannesburg, South Africa

[2]National Metrology Institute of South Africa, Pretoria, South Africa

Correspondence to:
Ronnie Kritzinger

Email:
ronniekritzinger@telkomsa.net

Postal address:
PO Box 2515, Noordheuwel 1756, Krugersdorp, South Africa

Dates:
Received: 11 Aug. 2010
Accepted: 24 Feb. 2011
Published: 13 May 2011

How to cite this article:
Kritzinger R, Meyer J, Burger J. Investigation of the power coupling of novel wavelength-selective couplers incorporating axially symmetric long-period fibre gratings. S Afr J Sci. 2011;107(5/6), Art. #400, 7 pages. doi:10.4102/sajs.v107i5/6.400

Evanescent-field coupling was studied experimentally in novel optical-fibre-based wavelength-selective couplers, using axially symmetric long-period fibre grating (LPFG) structures. The coupling characteristics of a wavelength-selective coupler at the resonant wavelength were investigated for different LPFG offset distances. It was shown that the wavelength-selective couplers effectively transferred light power at the LPFG resonant wavelength from one fibre to another. The performance of the couplers was consistent with simulations performed in MATLAB using coupled-mode theory.

Introduction

The rapid growth of the optical communications industry has compelled researchers to optimise data transmission over long-haul fibre optic links, and to develop low-cost fibre optic components, such as optical add-drop multiplexers that manage multiple wavelength channels and exhibit low insertion loss. Moreover, as data rates increase beyond 40 Gb/s in wavelength-division multiplexing networks as a result of the introduction of broadband technologies, the need for optical add-drop multiplexers that are economically viable and exhibit low loss increases because individual or multiple wavelengths carrying data channels are routed to and from a transmission fibre. Long-period fibre gratings and fibre Bragg gratings are in-fibre optical filters that contribute greatly to the wavelength-division multiplexed optical communications and sensing industry.[1,2] It has been shown that optical filters can be used to perform optical add-drop multiplexing.[1] A common optical add-drop multiplexer configuration consists of an optical circulator connected to a Bragg grating; this configuration exhibits low insertion loss (~2 dB), but the configuration is too expensive because of the high cost of circulators.[3] A 4-port 50% coupler with a Bragg grating connected to one of the coupler's outputs could also be used, but this configuration has unacceptably high insertion loss.[4]

Other optical add-drop multiplexer designs use evanescent coupling of light between a pair of fibres within a tapered region of a fused coupler.[5,6] These devices are difficult to manufacture, because they require uniform and reproducible fusion of two fibres over the length of the coupling region. Over the years, it has been shown that a long-period fibre grating (LPFG) is an efficient wavelength-selective device.[7,8] It is known that an LPFG structure is a periodic perturbation of the refractive index in a single-mode fibre (SMF), which causes a guided-to-cladding mode power exchange to occur at a certain wavelength.[9] When the forward propagating core mode interacts with the LPFG structure, the guided mode couples to several forward propagating cladding modes.[1,9] In addition to their low back reflection and low insertion loss, LPFGs are easy to fabricate because of a grating period that is normally several hundreds of micrometers.[1] It has been shown that the placement of two identical LPFGs in parallel and in close proximity results in the light at some wavelengths being rejected by one LPFG but collected again by the other LPFG.[8,10] The outputs from the two LPFGs are complementary to each other, one showing band-pass characteristics and the other showing band-rejection characteristics. Recently it has been shown that the coupling efficiency of a wavelength selective coupler (WSC) consisting of two parallel LPFGs is independent of the fibre orientation for CO_2 laser-induced LPFGs written in boron co-doped fibre.[11] CO_2-laser fabrication of LPFGs is more flexible than the traditional UV-fabrication of LPFGs and can be applied to almost any untreated glass fibres.[11] Four-port and six-port WSCs consisting of two and three parallel LPFGs, respectively, have been demonstrated.[7,12,13]

In this paper, theoretical and experimental results are presented of a narrowband wavelength-selective coupler consisting of two parallel, axially symmetric LPFGs fabricated with a CO_2 laser. Experimental results of a broadband WSC are also presented. Coupled-mode theory is used to model WSCs and the conditions for achieving efficient power transfer between the LPFGs are

identified and discussed. The experimental set-up that was developed to construct the WSCs is also presented. To our knowledge, this is the first time that the properties of WSC devices incorporating axially symmetric LPFGs fabricated with a custom CO_2 laser have been studied in detail.

Wavelength-selective coupler incorporating LPFGs

Principle of operation

Figure 1 illustrates a WSC consisting of two parallel SMFs, each consisting of identical uniform LPFGs. The fibres are separated by a distance (d) and are offset by a distance (z_1) in the direction of wave propagation. Light is launched into one of the fibres, called the transmission fibre, where the LPFG couples the light from the guided mode to the cladding mode of the fibre at a desired resonant wavelength. The phase-matching condition for the mode-coupling occurring in an LPFG structure is given by:

$$2\bar{s}_1 - \bar{S} \equiv -\bar{s}_f, \qquad \text{[Eqn 1]}$$

where $\bar{s}_1$ is the detuning parameter, $\bar{s}_f = 2\pi / \Lambda_{LPFG}$ is the grating wave vector, Λ_{LPFG} is the grating period, and $\bar{S}$ is the difference between the propagation constant of the guided core mode and the kth order cladding mode.[14] The resonant wavelength of the kth order cladding mode is given by:

$$\lambda_{LPFG}^{(k)} = (n_{co} - n_{cl}^{(k)})\Lambda_{LPFG}, \qquad \text{[Eqn 2]}$$

where n_{co} is the effective refractive index of the core mode and $n_{cl}^{(k)}$ is the effective refractive index of the kth order cladding mode (i.e. LP_{0k}).[9,14] Our theoretical analysis is based on the weakly guiding fibre approximation, where the refractive index difference between the core and cladding is very low.[14,15]

In the vicinity of an LPFG, the fundamental core mode (i.e. LP_{01}) couples to several co-propagating cladding modes.[14] The only cladding modes (LP_{mk} or HE_{1k}) to which the guided core mode can couple are those that exhibit azimuthally symmetric intensity profiles with central peaks, where $m = 0$ and $k = (1, 2, 3,..)$.[16,17] In Figure 1, the cladding mode

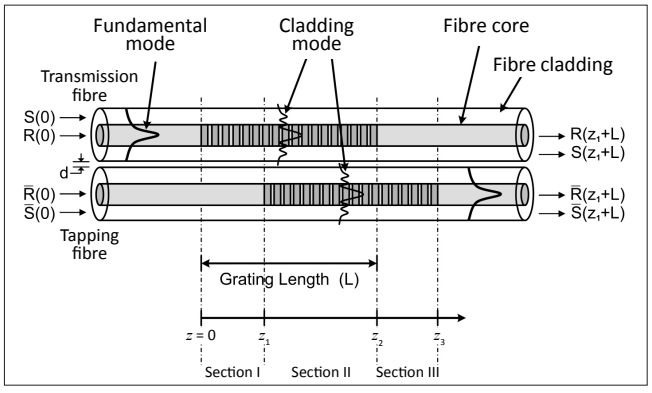

FIGURE 1: Schematic diagram of a wavelength-selective coupler consisting of two parallel fibres, each containing identical uniform long-period fibre gratings and displaced by an offset distance, z_1.

propagates in the cladding and excites a similar cladding mode in the tapping fibre, through evanescent-field coupling between the two fibres.[8] The LPFG in the tapping fibre then couples the cladding mode to the core mode. Only light at the resonant wavelength of the LPFGs will be coupled from the transmission fibre to the tapping fibre. The resonant light will be dropped into the tapping fibre and the non-resonant light will keep propagating in the transmission fibre, as shown in Figure 1. Another WSC should be arranged in reverse order to add a wavelength channel.[7] The coupling efficiency of the coupler is given by:

$$\eta = |\bar{R}(z_3)|^2 / |\bar{R}(0)|^2, \qquad \text{[Eqn 3]}$$

where $\bar{R}(0)$ is the input power launched into the transmission fibre and $\bar{R}(z_3)$ is the output power from the tapping fibre.[12] It has been shown that the coupling efficiency of the WSC can be maximised by introducing a finite offset between the LPFGs to increase the interaction length for evanescent-field coupling between the fibres and by using a suitable surrounding refractive index to expand the field distribution for better overlap with the other fibre.[11,12]

Dependence of coupling coefficients on cladding mode order and surrounding refractive index

To understand the coupling processes within a WSC, it is important to solve the coupled-mode equations derived for a WSC. Chiang et al.[12] provide a detailed theoretical analysis of a WSC consisting of identical uniform LPFGs. The coupling processes in the LPFG coupler are governed by the coupling coefficients K and C. The coupling coefficient K characterises an LPFG and serves as a measure of the power transfer between the LP_{01} and LP_{0k} mode, as a result of the mutual overlap of the fields in the core area (where the coupling perturbation in the form of a refractive index modulation is situated).[1,9] The coupling coefficient K can be adjusted by controlling the index modulation during LPFG fabrication.[1] On the other hand, the coupling coefficient C characterises the evanescent-field coupling between two parallel fibres in a WSC and measures the spatial overlapping of the two LP_{0k} mode fields over the cross-sectional area of one of the fibres.[12] The coupling coefficient C is defined as:

$$C = \frac{2\Delta}{\rho}\frac{U^2}{V^3}\frac{K_0[2+d/\rho]}{K_1^2(W)}, \qquad \text{[Eqn 4]}$$

where ρ is the cladding radius and Δ is the normalised index difference between the cladding and surrounding medium defined as $(n_2^2 - n_3^3)/2n_2^2$. The refractive index of the core, cladding and ambient region are denoted as n_1, n_2 and n_3, respectively. In Eqn 4, K_0 and K_1, are the modified Bessel functions and the normalised parameters V, U and W are defined as:

$$V = \frac{2\pi\rho}{\lambda_{LPFG}}\sqrt{n_2^2 - n_3^2}, \qquad \text{[Eqn 5]}$$

$$U = \frac{2\pi\rho}{\lambda_{LPFG}}\sqrt{n_2^2 - (n_{cl}^{(k)})^2} \qquad \text{[Eqn 6]}$$

and

$$W = \frac{2\pi\rho}{\lambda_{LPFG}} \sqrt{(n_{cl}^{(k)})^2 - n_3^2}. \quad \text{[Eqn 7]}$$

In this paper, theoretical results are presented for a WSC consisting of two identical uniform LPFG structures. For all the calculations, the fibre parameters of PS1500 fibre were used.[18] PS1500 fibre is a germanium-boron co-doped photosensitive SMF produced by Fibercore Ltd (Southampton, UK). The numerical aperture of the fibre is 0.13 and the LPFGs exhibit a grating period of 330 µm. When a WSC is produced, it is important that the fibre separation (d) is kept as small as possible (< 5 µm). During the theoretical analysis it is assumed that the fibres are touching, that is $d = 0$. Unless otherwise stated, the refractive index that surrounds the fibre can be taken as 1 (corresponding to a vacuum). It has been shown that the coupling coefficient C and the coupled-mode equations are accurate, even if the fibres in the WSC are touching.[10,12] Figure 2 illustrates the theoretical dependence of the coupling coefficient C on the cladding mode order at a resonant wavelength of 1550 nm for five different surrounding indices. In Figure 2 it is shown that the coupling coefficient C can be increased by using a suitable surrounding index (n_3) and a higher-order cladding mode. Figure 3a illustrates the dependence of the coupling coefficient C on the surrounding refractive index for the LP_{07} cladding mode. The grating length is 25 mm and the resonant wavelength is 1550 nm for coupling to the LP_{07} cladding mode when $n_3 = 1$. In Figure 3a, it can be seen that the coupling coefficient C increases as the surrounding index is increased. However, as the surrounding index becomes really close to the cladding index (n_2), the cladding mode becomes more weakly confined in the fibre until the guiding is totally lost and coupling becomes undefined.[11,12]

The shape of the curve in Figure 3a illustrates that the coupling coefficient C becomes very sensitive to changes in the refractive index as the surrounding index becomes very close to the cladding index, which is in agreement with earlier work.[12] The coupling coefficient K remains insensitive to the change in the surrounding index unless the surrounding index becomes very close to the cladding index.[12] Figure 3b illustrates that the resonant wavelength increases with surrounding index (n_3) and the rate of wavelength shift increases as the surrounding index approaches the cladding index.[19,20] Figure 4 illustrates the dependence of the coupling coefficient C on the surrounding index for the LP_{07} cladding mode as the fibre separation (d) is increased. It is shown that the fibre separation influences the coupling coefficient C tremendously. In practice, it is important to keep the fibre separation to a minimum.

Experimental set-up

Figure 5 illustrates the unique experimental set-up used for WSC characterisation. This set-up enables one to easily measure physical properties of a WSC in a very flexible manner as part of the characterisation process, as opposed to miniature but inflexible fixtures that could be encountered in device packaging.[21,22] It should be noted that the schematic of

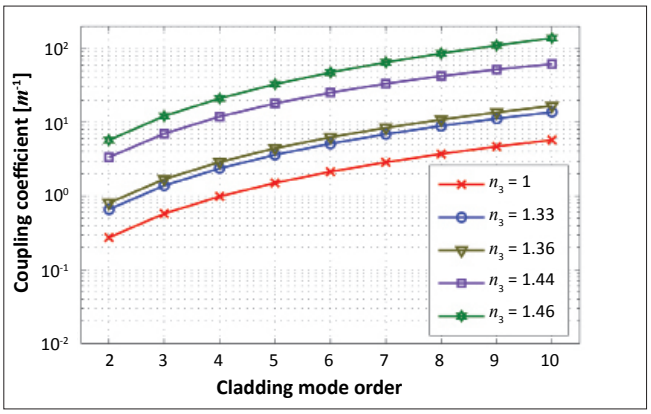

FIGURE 2: Dependence of the coupling coefficient C on the cladding mode order and the surrounding index (n_3) at the resonant wavelength for two fibres touching.

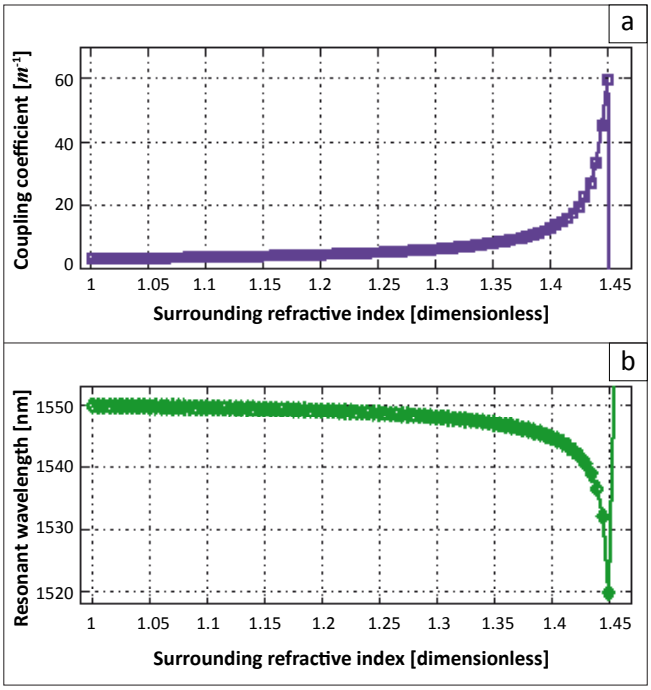

FIGURE 3: Dependence of the coupling coefficient C and the resonant wavelength on the surrounding refractive index for the LP_{07} cladding mode.

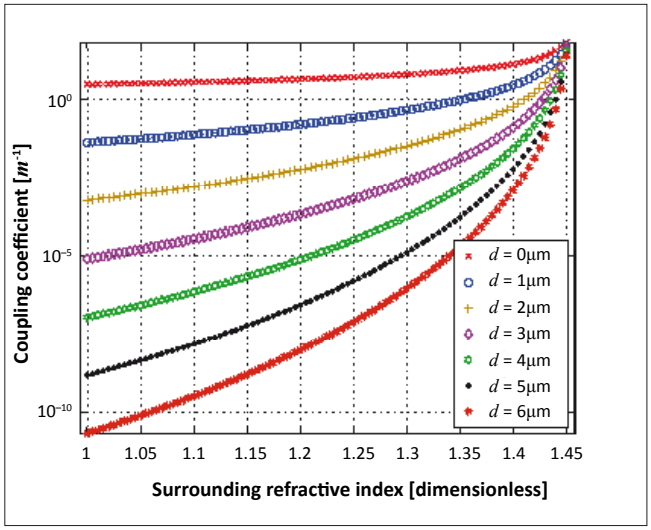

FIGURE 4: Dependence of the coupling coefficient C on the surrounding index for the LP_{07} cladding mode as the fibre separation (d) is increased.

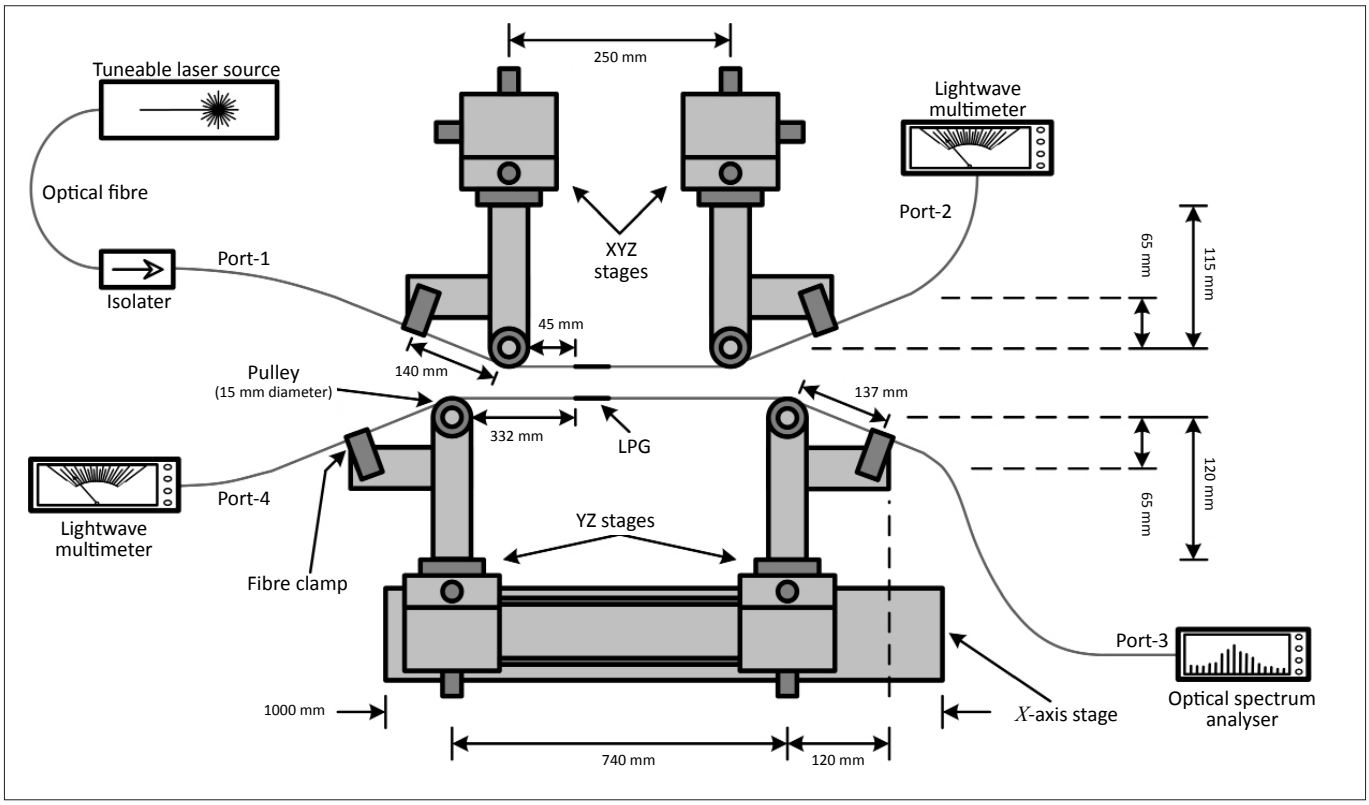

FIGURE 5: Schematic layout of the experimental set-up used to construct a wavelength-selective coupler consisting of long-period fibre gratings.

the experimental set-up has not been drawn to scale and the measurements shown are for convenience.

The WSC consists of two identical azimuthally symmetric LPFGs, which are placed in parallel in close contact, without the need for fusion. The WSC was constructed in such a manner that the fibres lay in a horizontal position. To minimise the vibration that might influence the performance of the WSC during experiments, the experimental set-up was assembled on a vibration-isolated table and air turbulence was avoided. In Figure 5, the transmission fibre is connected to the tuneable laser source and the tapping fibre is connected to the optical spectrum analyser. The transmission fibre and tapping fibre are fixed on separate translation stages, such that the two parallel fibres could be aligned to each other. Two microscopes are used to align the fibres along the *x*-axis and one microscope is used to align the fibres along the *y*-axis. Translation stages that support the transmission fibre operate independently from the stages for the tapping fibre. However, the translation stages that support the tapping fibre are affixed to a common base, which is mounted on an *x*-axis translation stage. This *x*-axis translation stage can be moved a maximum distance of 100 mm. Each fibre was inspected to ensure that the entire section of fibre between the fibre clamps was stripped from its protective coating. The fibres were chemically stripped using dichloromethane, after which they were cleaned using acetone and propanol. Before the fibres were permanently fixed between the fibre clamps and connected to measurement equipment, the fibres were again chemically cleaned using acetone, propanol and a pressure duster. When the transmission fibre and tapping fibre were fixed in the experimental set-up, the LPFGs were analysed and the resonant wavelengths retrieved. A tungsten-halogen broadband source (Ocean Optics LS-1, Ocean Optics Corporation, Dunedin, FL, USA) was used as the light source and an optical spectrum analyser (Yokogawa AQ6317C, Yokogawa Electric Corporation, Tokyo, Japan) was used to measure the output spectrum of each LPFG. During the experiments, a wavelength-tuneable laser source (Agilent 81600B, Agilent Technologies Inc., Santa Clara, CA, USA) was used as a light source and was connected to Port 1 as illustrated in Figure 5. An optical isolator was used in conjunction with the wavelength-tuneable laser source to protect the laser source from any back reflection that might exist in the system. An optical spectrum analyser (Yokogawa AQ6317C) was connected to Port 3, as illustrated in Figure 5, to measure the light power coupled to the tapping fibre. Any optical power routed to Port 2 and Port 4 was measured with a lightwave multimeter (Agilent 8163A). Fibre links used between the various components in the experimental set-up were kept as short as possible in order to minimise insertion losses.

Experimental results

Narrowband wavelength-selective coupler

The WSC consists of two identical uniform LPFGs fabricated in an axially symmetric manner using a CO_2 laser. The experimental set-up introduced in Kritzinger et al.[23] was used to fabricate the LPFGs in PS1500 SMF[18] by implementing the point-by-point fabrication method. The gratings exhibited a period of 325 μm and a total length of 25 mm. The gratings were placed in the WSC experimental set-up and brought together using the translation stages illustrated in Figure 5.

Suitable tension was applied along the fibres to keep them in close parallel contact. The transmission spectrum of the LPFGs is illustrated in Figure 6.

In Figure 6, LPFG 1 corresponds to the LPFG fabricated in the transmission fibre and LPFG 2 corresponds to the LPFG fabricated in the tapping fibre. The resonant wavelengths (λ_{LPFG}) of the first and second LPFG at the LP_{07} -mode attenuation peak were 1520.3 nm and 1521.4 nm, respectively. The resonant wavelengths were measured when the fibres were surrounded by air. The contrast of the first and second LPFG at λ_{LPFG} for the LP_{07} -mode was 4.9 dB and 4.0 dB, respectively, and corresponded to a coupling coefficient K of 38.2 m^{-1} and 36.7 m^{-1}, respectively. The LPFG in the transmission fibre coupled approximately 68% of light power into the cladding at λ_{LPFG} for the LP_{07} -mode. The rest of the light power was routed in the fibre core to Port 2 of the WSC illustrated in Figure 5. The 3-dB bandwidths of the first and second LPFG for the LP_{07}-mode were 16.0 nm and 12.6 nm, respectively. In the experimental set-up, the gratings were initially aligned such that the offset distance (z_1) was zero. During the experiments, the surrounding refractive index was increased by applying acetone (n_3 = 1.36 at 589.3 nm) to the fibre sections that contained the LPFGs. The variation of the coupling efficiency (η) at λ_{LPFG} with the offset distance is shown in Figure 7.

The resonant wavelength of the LPFGs shifted 3.3 nm to the shorter wavelength side when acetone was used to increase the surrounding index of the fibre. It was observed that the power output from the tapping fibre increased, with a corresponding shift in LPFG resonant wavelength, as the surrounding refractive index of the fibres was increased. The power coupled from the transmission fibre to the tapping fibre increased as the surrounding refractive index became larger, because the field distribution of the LP_{07} -mode was broadened, resulting in larger field overlap with the other fibre.[11] The experimental measurements agreed well with the theoretical prediction when the fibre separation (d) was set to 3 μm in the simulation, as shown in Figure 7. Deviations from the theoretical prediction could be because of some small lateral angular relative shifts between fibres and effectively a change in coupling as the fibres were translated with respect to each other. Furthermore, close proximity of the fibres became more challenging as the coupling distance was enlarged, because greater parallelism and simultaneous close spacing of fibres were needed. It was confirmed with a microscope that the fibre separation was smaller than 4 μm at each offset distance. Figure 8 illustrates an image of the transmission fibre and tapping fibre in the region of the first LPFG when the offset distance was 70 mm.

When 1 mW at 1517 nm was injected into Port 1 of the WSC for z_1 = 70 mm, the power measured at Port 2, Port 3 and Port 4 was 296.1 ± 0.1 μW, 11.7 ± 0.8 μW and 95.3 ± 0.2 nW, respectively. The coupling efficiency measured at z_1 = 70 mm with a surrounding refractive index of 1.36 was -19.3 ± 0.3 dB, which corresponded to a power conversion efficiency of 1.2 ± 0.1%. An extrapolation of Figure 7 indicates that the efficiency could have been increased to approximately -13 dB if z_1 = 120 mm, which is beyond the translation range of the experimental set-up. The 3-dB bandwidth of the output spectrum of the tapping fibre was 0.05 nm. The narrowband WSC was 95 mm in length at a 70 mm offset distance. The excess loss (including splicing losses) of the WSC was ~69% (5.1 dB) and could predominantly be as a result of the high insertion losses present in the WSC. The directivity of the WSC was greater than 40 dB, because the coupler effectively filters out non-resonant light.[7] The coupling efficiency could be increased further by: (1) increasing the offset distance, (2) bringing the fibres closer together or (3) etching the claddings

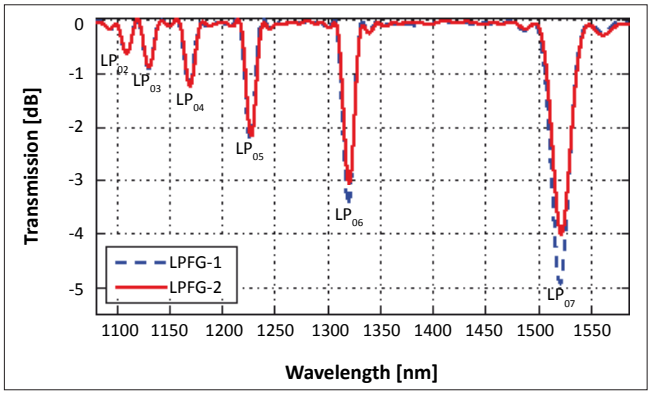

FIGURE 6: Transmission spectrum of 25 mm uniform long-period fibre gratings (LPFGs) fabricated axially symmetric in separate single-mode fibres using a CO_2 laser. The transmission spectrum is shown in the wavelength region where mode-coupling occurs to the seven lower-order cladding modes.

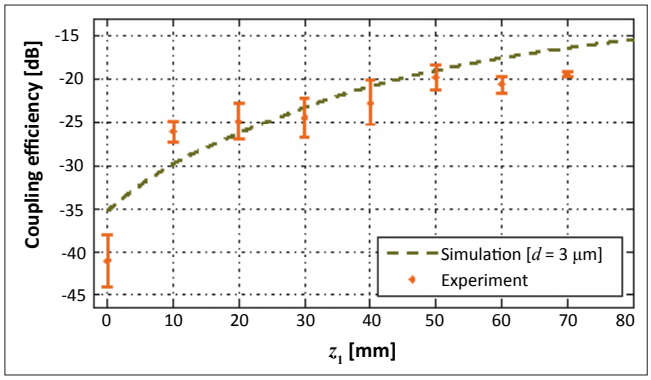

Error bars represent standard deviation.

FIGURE 7: Variation of the coupling efficiency of the narrowband wavelength-selective coupler at the resonant wavelength with offset distance, z_1.

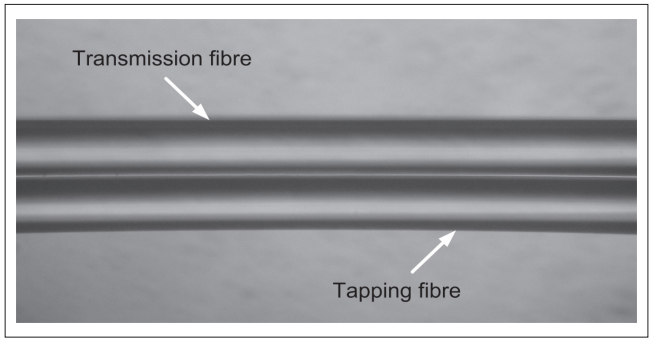

The image was captured through a microscope with a 4 megapixel Canon digital camera.

FIGURE 8: Image of the transmission fibre and tapping fibre in the region of the first long-period fibre grating when z_1 = 70 mm.

of the fibres. Table 1 lists the performance specifications of the WSC for $n_3 = 1.36$.

Broadband wavelength-selective coupler

The WSC consists of two identical non-uniform LPFGs, fabricated axially symmetric using a CO_2 laser. The LPFGs were designed using a genetic algorithm for a flat, broad stopband characteristic for multichannel tapping and also fabricated in PS1500 SMF.[18] The gratings exhibited a length of 40 mm and a period of 457 µm in the central region of each grating. The transmission spectrum of the non-uniform LPFG structures is illustrated in Figure 9. In Figure 9, LPFG 1 again corresponds to the LPFG fabricated in the transmission fibre and LPFG 2 corresponds to the LPFG fabricated in the tapping fibre.

The resonant wavelengths of the first and second LPFGs at the LP_{05}-mode attenuation peak were 1561.9 nm and 1561.3 nm, respectively, when measured in air. The contrast of the first and second LPFGs at the resonant wavelength (λ_{LPFG}) for the LP_{05}-mode was 9.3 dB and 9.4 dB, respectively, and corresponded to a coupling coefficient K of ~12.1 cm^{-1}. The LPFG in the transmission fibre coupled approximately 88% of light power into the cladding at λ_{LPFG} for the LP_{05}-mode. The 3-dB bandwidth of the first and second LPFGs for the LP_{05}-mode were 36.0 nm and 37.8 nm, respectively. During the experiments, acetone was again applied to the fibre sections that contained the LPFGs to increase the surrounding index. The variation of the coupling efficiency at λ_{LPFG} with the offset distance is shown in Figure 10.

When acetone was used to increase the surrounding refractive index of the fibre, the resonant wavelengths of the LPFGs shifted 4.1 nm to the shorter wavelength side. The power output from the tapping fibre again increased as the surrounding refractive index of the fibres was increased. As shown in Figure 10, the experimental results agreed well with the theoretical results when the fibre separation (d) was set to 3 µm in the simulation. From the theoretical predictions, deviations can again be understood to be of a nature similar to that of the narrow bandwidth WSC. As in the case of the narrowband WSC, the fibre separation at each offset distance was observed to be smaller than 4 µm. When 1 mW of light with a wavelength 1557.5 nm was injected into Port 1 of the WSC for $z_1 = 60$ mm, the power measured at Port 2, Port 3 and Port 4 was 111.2 ± 0.1 µW, 9.6 ± 0.7 µW and 123.3 ± 0.3 nW, respectively. The maximum coupling efficiency, measured at $z_1 = 60$ mm with a surrounding refractive index of 1.36, was -20.2 ± 0.3 dB, which corresponded to a power conversion efficiency of 0.95 ± 0.07%. The coupling efficiency of the broadband WSC was almost the same as that obtained with the narrowband WSC. However, during the experiments, mode-coupling was only performed between the fundamental mode and the LP_{05} cladding mode and therefore the value of the coupling coefficient C during this experiment was much lower than when it was compared to the narrowband WSC experiment. Longer LPFGs were manufactured for the WSC, to increase the transmission loss of each grating.[1] By using longer grating lengths in the broadband WSC, it was possible

TABLE 1: Performance specifications of the narrowband wavelength-selective coupler.

Parameter	Value
Centre wavelength [nm]	1517
Bandwidth [nm]	13
Coupling ratio [%]	3.8 ± 0.3
Insertion loss (Port 1→Port 2) [dB]	5.286 ± 0.003
Insertion loss (Port 1→Port 3) [dB]	19.3 ± 0.3
Excess loss [dB]	5.12 ± 0.02
Polarisation-dependent loss [dB]	< 3.7
Directivity [dB]	> 40

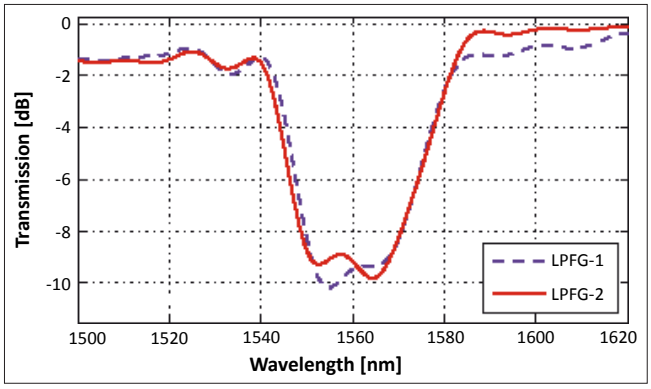

FIGURE 9: Transmission spectrum of 40 mm non-uniform long-period fibre gratings (LPFGs) fabricated axially symmetric in separate single-mode fibres using a CO_2 laser. The LPFGs were designed using a genetic algorithm.

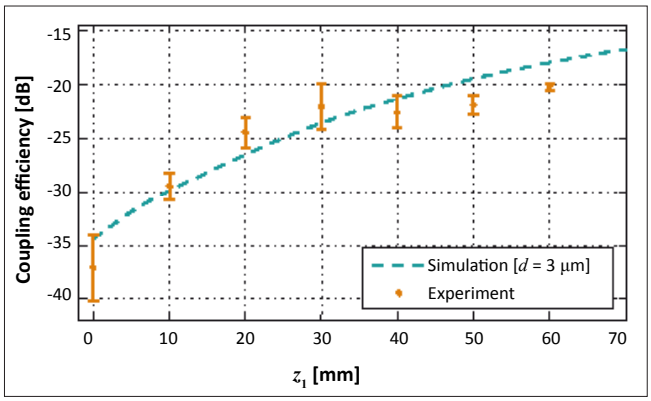

Error bars represent standard deviation.

FIGURE 10: Variation of the coupling efficiency of the broadband wavelength-selective coupler at the resonant wavelength with offset distance, z_1.

to effectively couple more light power into the cladding and to achieve a coupling efficiency close to that of the narrowband WSC. The broadband WSC was 100 mm in length when maximum coupling efficiency was achieved. The excess loss of the broadband WSC was ~88% (9.2 dB), mainly as a result of insertion losses. The directivity of the broadband WSC was greater than 38 dB. During these experiments, the interaction length between the LPFGs could not be increased further because of limitations on the experimental set-up. Table 2 lists the performance specifications of the broadband WSC for $n_3 = 1.36$.

Conclusion

In this paper, narrowband and broadband WSCs that consisted of axially symmetric LPFGs fabricated with a CO_2 laser

TABLE 2: Performance specifications of the broadband wavelength-selective coupler.

Parameter	Value
Centre wavelength [nm]	1558
Bandwidth [nm]	36
Coupling ratio [%]	8.0 ± 0.6
Insertion loss (Port-1→Port-2) [dB]	9.54 ± 0.01
Insertion loss (Port-1→Port-3) [dB]	20.2 ± 0.3
Excess loss [dB]	9.18 ± 0.05
Polarisation-dependent loss [dB]	< 4.8
Directivity [dB]	> 38

were described. The operation of a WSC was demonstrated and the coupler was characterised. The dependence of the coupling coefficients on cladding mode order, fibre separation and surrounding refractive index were discussed. The WSCs constructed effectively transferred light power at the LPFG resonant wavelength from one fibre to another, but did not exhibit a high coupling efficiency. It was shown that the fibres in the WSCs did not touch, which subsequently influenced the coupling efficiency significantly. Although the WSCs exhibited high insertion loss, they effectively filtered out non-resonant light. To optimise the WSCs, a study could be conducted on increasing the coupling efficiency of a WSC further by bringing the fibres closer together by using a different experimental set-up, increasing the ambient index or by etching the claddings of the fibres. WSCs show great promise as channel routing devices in a wavelength-division multiplexing network, which could be used in the de-multiplexing or multiplexing part of an optical add-drop multiplexer.

Acknowledgements

The research described in this paper was financially supported by CBI Electric (Pty) Ltd, Ericsson South Africa (Pty) Ltd, Telkom (Pty) Ltd, the National Laser Centre, THRIP, the National Research Foundation and the University of Johannesburg. Ronnie Kritzinger wishes to thank Johan Burger of NMISA for his guidance and support throughout this project.

References

1. Kashyap R. Fibre Bragg gratings. New York: Academic Press; 1999.
2. James SW, Tatam RP. Optical fibre long-period grating sensors: Characteristics and application. Meas Sci Technol. 2003;14:R49–R61. doi:10.1088/0957-0233/14/5/201
3. Giles CR, Mizrahi V. Low-loss add/drop multiplexers for WDM lightwave networks. Paper presented at: IOOC 1995. Proceedings of the International Conference on Integrated Optics and Optical Fiber Communication; 1995 June 26–30; Hong Kong, China. Hong Kong: Chinese University Press; 1995. p. 66–67.
4. Kashyap R, Armitage JR, Wyatt R, Davey ST, Williams DL. All-fibre narrowband reflection gratings at 1500 nm. Electron Lett. 1990;26:730–731. doi:10.1049/el:19900476
5. Kewitsch AS, Rakuljic GA, Willems PA, Yariv A. All-fiber zero-insertion-loss add drop filter for wavelength-division multiplexing. Opt Lett. 1998;23:106–108. doi:10.1364/OL.23.000106, PMid:18084427
6. Baumann I, Seifert J, Nowak W, Sauer M. Compact all-fiber add-drop-multiplexer using fiber Bragg gratings. IEEE Photonics Technol Lett. 1996;8:1331–1333. doi:10.1109/68.536645
7. Grubsky V, Starodubov S, Feinberg J. Wavelength-selective coupler and add/drop multiplexer using long-period fibre gratings. Paper presented at: OFC 2000. Proceedings of the Optical Fiber Communication Conference; 2000 March 7–10; Baltimore, USA. New York: IEEE Xplore Digital Library; 2000. p. 28–30.
8. Chiang KS, Liu Y, Ng MN, Li S. Coupling between two parallel long-period fibre gratings. Electron Lett. 2000;36:1408–1409. doi:10.1049/el:20001014
9. Vengsarkar AM, Lemaire PJ, Judkins JB, Bhatia V, Erdogan T, Sipe JE. Long-period fibre gratings as band-rejection filters. J Lightwave Technol. 1996;14:58–65. doi:10.1109/50.476137
10. Zhu Y, Chao L, Lacquet BM, Swart PL. Wavelength-tuneable add/drop multiplexer for DWDM using long-period gratings and fibre stretchers. Opt Commun. 2002;208:337–344. doi:10.1016/S0030-4018(02)01634-6
11. Liu Y, Chiang KS, Rao YJ, Ran ZL, Zhu T. Light coupling between two parallel CO_2-laser written long-period fiber gratings. Opt Express. 2007;15:17645–17651. doi:10.1364/OE.15.017645, PMid:19551060
12. Chiang KS, Chan FYM, Ng MN. Analysis of two parallel long-period fiber gratings. J Lightwave Technol. 2004;22:1358–1366. doi:10.1109/JLT.2004.825357
13. Liu Y, Chiang KS. Broadband optical coupler based on evanescent-field coupling between three parallel long-period fiber gratings. IEEE Photonics Technol Lett. 2006;18:229–231. doi:10.1109/LPT.2005.861534
14. Erdogan T. Fibre grating spectra. J Lightwave Technol. 1997;15:1277–1294. doi:10.1109/50.618322
15. Keiser G. Optical fiber communications. Singapore: McGraw-Hill; 2000.
16. Buck JA. Fundamentals of optical fibre. New York: Wiley; 1995.
17. Shu X, Zhang L, Bennion I. Sensitivity characteristics of long-period fibre gratings. J Lightwave Technol. 2002;20:255–266. doi:10.1109/50.983240
18. Fibercore Limited. PS1250/1500 Photosensitive SMF: Product factnote [document on the Internet]. c2009 [cited 2009 June 5]. Available from: http://www.fibercore.com/Portals/0/PropertyAgent/412/Files/12/PS%20Fiber.pdf
19. Patrick HJ, Kersey AD, Bucholtz F. Analysis of the response of long-period fiber gratings to external index of refraction. J Lightwave Technol. 1998;16:1606–1612. doi:10.1109/50.712243
20. Chiang KS, Liu Y, Ng MN, Dong X. Analysis of etched long-period fibre gratings and its response to external refractive index. Electron Lett. 2000;36:966–967. doi:10.1049/el:20000701
21. Grubsky V and Starodubov D, inventors; Sabeus Photonics, assignee. Wavelength-selective optical fiber components using cladding-mode assisted coupling. United States patent 6360038. 2002 Mar 19.
22. Xu J, inventor; Aster Corporation, assignee. Fiber optic coupler. United States patent 4923268. 1990 May 8.
23. Kritzinger R, Schmieder D, Booysen A. Azimuthally symmetric long-period fibre grating fabrication with a TEM_{01}-mode CO_2 laser. Meas Sci Technol. 2009;20(3):034004. doi:10.1088/0957-0233/20/3/034004